JOC Article

Fluorescent Pyrimidopyrimidoindole Nucleosides: Control of Photophysical Characterizations by Substituent Effects

Masahiro Mizuta,[†,§] Kohji Seio,[‡,§] Kenichi Miyata,[†,§] and Mitsuo Sekine*[,†,§]

Department of Life Science, Frontier Collaborative Research Center, Tokyo Institute of Technology, and CREST of JST, 4259 Nagatsuta, Midori-ku Yokohama, Japan

msekine@bio.titech.ac.jp

Received January 31, 2007

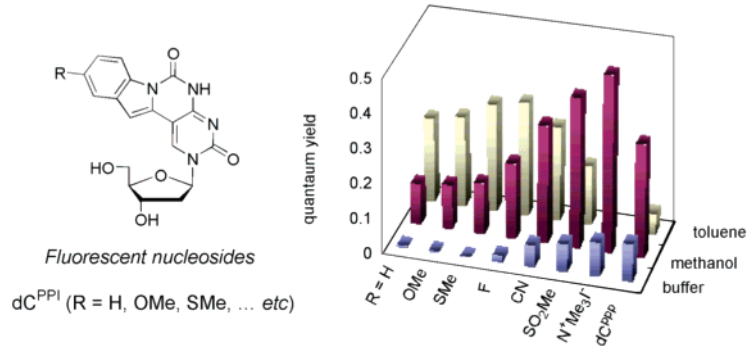

10-(2-Deoxy-β-D-ribofuranosyl)pyrimido[4′,5′:4,5]pyrimido[1,6-*a*]indole-6,9(7*H*)-dione (dC^{PPI}) and its derivatives were synthesized via the Suzuki−Miyaura coupling reaction of 5-iododeoxycytidine with 5-substituted *N*-Boc-indole-2-borates and characterized by UV−vis and fluorescence spectroscopy. The new fluorescent nucleosides showed rather large Stokes shifts (116−139 nm) in an aqueous buffer. The fluorescent intensities were dependent on the nature of the substituents on the indole rings. The electron-withdrawing groups increased the fluorescent intensity while the electron-donating groups having lone pairs decreased it. Among the substituted dC^{PPI} derivatives tested, the trimethylammonium derivative of dC^{PPI} was found to emit the brightest fluorescent light. The solvatochromism of dC^{PPI} and its derivatives was also studied. Some of the dC^{PPI} derivatives showed interesting solvent-dependent fluorescence enhancement and could be useful as new fluorescent structural probes for nucleic acids. The Lippert−Mataga analyses of the Stokes shift were also carried out to obtain estimated values of the dipole moment of the excited states of some of the derivatives.

Introduction

There have been reported a number of fluorescent nucleosides having an artificial nucleobase imitating the natural DNA bases.[1] These fluorescent nucleosides have been used to study the structures of nucleic acids[2] and their biological functions such as replication, transcription, recombination, and repair, because they minimally perturb the DNA structure.[3]

Among them, 2-aminopurine (2-AP) nucleoside derivatives are the most popular.[4] 2-AP has a high quantum yield (0.68) at a physiological pH and can be selectively excited by light of lower energy in comparison to the natural nucleic acid bases.

[†] Department of Life Science.
[§] CREST.
[‡] Frontier Collaborative Research Center.

(1) (a) Millar, D. P. *Curr. Opin. Struct. Biol.* **1996**, *6*, 322−326. (b) Wojczewski, C.; Stolze, K.; Engels, J. W. *Synlett* **1999**, 1667−1678. (c) Hawkins, M. E. *Cell Biochem. Biophys.* **2001**, *34*, 257−281. (d) Murphy, C. J. *Adv. Photochem.* **2001**, *26*, 145−217. (e) Rist, M. J.; Marino, J. P. *Curr. Org. Chem.* **2002**, *6*, 775−793. (f) Hawkins, M. E. *Top. Fluoresc. Spectrosc.* **2003**, *7*, 151−175. (g) Ranasinghe, R. T.; Brown, T. *Chem. Commun.* **2005**, 5487−5502. (h) Okamoto, A.; Saito, Y.; Saito, I. *J. Photochem. Photobiol. C* **2005**, *6*, 108−122. (i) Wilson, J. N.; Kool, E. T. *Org. Biomol. Chem.* **2006**, *4*, 4265−4274.

(2) (a) Nordlund, T. M.; Andersson, S.; Nilsson, L.; Rigler, R.; Graeslund, A.; McLaughlin, L. W. *Biochemistry* **1989**, *28*, 9095−9103. (b) Guest, C. R.; Hochstrasser, R. A.; Sowers, L. C.; Millar, D. P. *Biochemistry* **1991**, *30*, 3271−3279. (c) Roberts, R. J. *Cell* **1995**, 82, 9−12. (d) Millar, D. P. *Curr. Opin. Struct. Biol.* **1996**, *6*, 322−326. (e) Jiao, Y.; Stringfellow, S.; Yu, H. *J. Biomol. Struct. Dyn.* **2002**, *19*, 629−634. (f) Greco, N. J.; Tor, Y. *J. Am. Chem. Soc.* **2005**, *127*, 10784−10785. (g) Tinsley, R. A.; Walter, N. G. *RNA* **2006**, *12*, 522−529. (h) Kim, S. J.; Kool, E. T. *J. Am. Chem. Soc.* **2006**, *128*, 6164−6171. (i) Andreatta, D.; Sen, S.; Pèrez Lustres, J. L.; Kovalenko, S. A.; Ernsting, N. P.; Murphy, C. J.; Coleman, R. S.; Berg, M. A. *J. Am. Chem. Soc.* **2006**, *128*, 6885−6892.

10.1021/jo070206j CCC: $37.00
Published on Web 06/08/2007

For example, 2-AP has been used to obtain circumstantial evidence of base flipping in the target lesion of DNA photolyase, a DNA binding protein, that repairs pyrimidine photodimers.[5]

Other commercially available fluorescent base analogues are pteridines, 3-methylisoxanthopterin (3MI),[6] and 6-methylisoxanthopterine (6MI),[7] which can be used as guanine analogues. Both analogues also have the absorbance maxima which are red-shifted in comparison to those of the naturally occurring nucleic acids.

In addition to these fluorescent purine analogues, there have been reported several fluorescent pyrimidine analogues. For example, Saito et al. reported the synthesis and fluorescent properties of benzopyridopyrimidine nucleoside (BPP)[8] and demonstrated the discrimination of BPP-A and BPP-G base pairs in DNA duplexes by detecting the quenching of the fluorescence of BPP by nearby guanine bases. Another example is the tricyclic cytosine analogue, 3,5-diaza-4-oxophenothiazine (tC),[9] having high fluorescence quantum yield even after incorporation into single- and double-strands.

Recently, we also reported new fluorescent pyrimidine nucleosides of a bicyclic 4-*N*-carbamoyldeoxycytidine derivative (dC^{hpp})[10a] and a pyrrolopyrimidopyrimidine nucleoside (dC^{PPP}).[10b] Each had a rather strong fluorescence quantum yield of 0.11 in an aqueous buffer, and the fluorescence was quenched by addition of guanine.[10]

SCHEME 1. Synthesis of Pyrrolopyrimidopyrimidine Nucleoside (dC^{PPP})

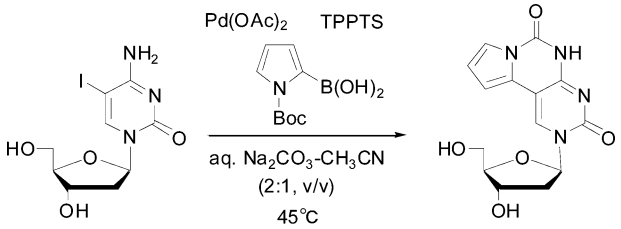

SCHEME 2. Structure of dC^{PPP} and dC^{PPI} Derivatives

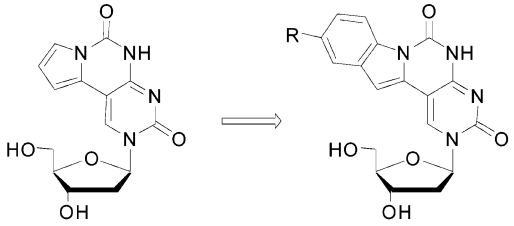

Although these fluorescent nucleoside derivatives have been well characterized, no papers have appeared on comprehensive studies on substituent effects of their core structures. It is well-established that the substituent in a fluorescent organic compound significantly influences its absorption and emission maxima, and quantum yields. There have been many papers on the substituent effect of various fluorophores such as coumarin,[11] naphthalene,[12] BODIPY,[13] thioxanthone,[14] imidazo[1,2-*a*]pyridine,[15] and imidazo[1,2-*a*]pyrazin-3(7*H*)-one[16] on the quantum yield. These studies showed that the fluorescent property could be successfully modulated by introduction of appropriate substituents.

In this paper, we report the synthesis and photophysical properties of a series of pyrimidopyrimidoindole nucleoside (dC^{PPI}) derivatives which are indole-type analogues of dC^{PPP}. We also studied the solvatochromic effects and pH dependence of their fluorescent properties and analyzed the relationship between these properties and the substituents. These solvent-dependent fluorescence properties indicated the usefulness of some of these fluorescent nucleosides as new structure probes of nucleic acids.

(3) (a) Frey, M. W.; Sowers, L. C.; Millar, D. P.; Benkovic, S. J. *Biochemistry* **1995**, *34*, 9185−92. (b) Stivers, J. T. *Nucleic Acids Res.* **1998**, *26*, 3837−3844. (c) Moser, A. M.; Patel, M.; Yoo, H.; Balis, F. M.; Hawkins, M. E. *Anal. Biochem.* **2000**, *281*, 216−222. (d) Deprez, E.; Tauc, P.; Leh, H.; Mouscadet, J. F.; Auclair, C.; Hawkins, M. E.; Brochon, J. C. *Proc. Natl. Acad. Sci. U.S.A.* **2001**, *98*, 10090−10095. (e) Wojtuszewski, K.; Hawkins, M. E.; Cole, J. L.; Mukerji, I. *Biochemistry* **2001**, *40*, 2588−2598. (f) Liu, C.; Martin, C. T. *J. Biol. Chem.* **2002**, *277*, 2725−2731. (g) Shipova, E.; Gates, K. S. *Bioorg. Med. Chem. Lett.* **2005**, *15*, 2111−2113. (h) Hariharan, C.; Reha-Krantz, L. J. *Biochemistry* **2005**, *44*, 15674−15684. (i) Hariharan, C.; Bloom, L. B.; Helquist, S. A.; Kool, E. T.; Reha-Krantz, L. J. *Biochemistry* **2006**, *45*, 2836−2844. (j) Srivatsan, S. G.; Tor, Y. *J. Am. Chem. Soc.* **2007**, *129*, 2044−2053.

(4) (a) Ward, D. C.; Reigh, E.; Stryer, L. *J. Biol. Chem.* **1969**, *244*, 1228−1237. (b) Sowers, L. C.; Fazakerley, G. V.; Erija, R.; Kaplan, B. E.; Goodman, M. F. *Proc. Natl. Acad. Sci. U.S.A.* **1986**, *83*, 5434−5438.

(5) (a) Rachofsky, E. L.; Seibert, E.; Stivers, J. T.; Osman, R.; Ross, J. B. A. *Biochemistry* **2001**, *40*, 957−967. (b) Christine, K. S.; MacFarlane, A. W., IV; Yang, K.; Stanley, R. J. *J. Biol. Chem.* **2002**, *277*, 38339−38344. (c) Roy, S. *Methods Enzymol.* **2003**, *370*, 568−576. (d) Hoffman, P. D.; Wang, H.; Lawrence, C. W.; Iwai, S.; Hanaoka, F.; Hays, J. B. *DNA Repair* **2005**, *4*, 983−993.

(6) (a) Hawkins, M. E.; Pfleiderer, W.; Balis, F. M.; Porter, D.; Knutson, J. R. *Anal. Biochem.* **1997**, *244*, 86−95. (b) Hawkins, M. E.; Balis, F. M. *Nucleic Acids Res.* **2004**, *32*, e62.

(7) (a) Seibert, E.; Ross, J. B. A.; Osman, R. *J. Mol. Biol.* **2003**, *330*, 687−703. (b) Roca, A. I.; Singleton, S. F. *J. Am. Chem. Soc.* **2003**, *125*, 15366−15375. (c) Shchyolkina, A. K.; Kaluzhny, D. N.; Borisova, O. F.; Hawkins, M. E.; Jernigan, R. L.; Jovin, T. M.; Arndt-Jovin, D. J.; Zhurkin, V. B. *Nucleic Acids Res.* **2004**, *32*, 432−440.

(8) (a) Okamoto, A.; Tainaka, K.; Saito, I. *J. Am. Chem. Soc.* **2003**, *125*, 4972−4973. (b) Okamoto, A.; Tainaka, K.; Saito, I. *Chem. Lett.* **2003**, *32*, 684−685. (c) Okamoto, A.; Tainaka, K.; Saito, I. *Photomed. Photobiol.* **2003**, *25*, 39−40.

(9) (a) Lin, K. Y.; Jones, R. J.; Matteucci, M. *J. Am. Chem. Soc.* **1995**, *117*, 3873−3874. (b) Eldrup, A. B.; Nielsen, B. B.; Haaima, G.; Rasmussen, H.; Kastrup, J. S.; Christensen, C.; Nielsen, P. E. *Eur. J. Org. Chem.* **2001**, *9*, 1781−1790. (c) Wilhelmsson, L. M.; Holmen, A.; Lincoln, P.; Nielsen, P. E.; Norden, B. *J. Am. Chem. Soc.* **2001**, *123*, 2434−2435. (d) Wilhelmsson, L. M.; Sandin, P.; Holmen, A.; Albinsson, B.; Lincoln, P.; Norden, B. *J. Phys. Chem. B* **2003**, *107*, 9094−9101. (e) Engman, K. C.; Sandin, P.; Osborne, S.; Brown, T.; Billeter, M.; Lincoln, P.; Norden, B.; Albinsson, B.; Wilhelmsson, L. M. *Nucleic Acids Res.* **2004**, *32*, 5087−5095. (f) Sandin, P.; Wilhelmsson, L. M.; Lincoln, P.; Powers, V. E. C.; Brown, T.; Albinsson, B. *Nucleic Acids Res.* **2005**, *33*, 5019−5025.

(10) (a) Miyata, K.; Tamamushi, R.; Ohkubo, A.; Taguchi, H.; Seio, K.; Santa, T.; Sekine, M. *Org. Lett.* **2006**, *8*, 1545−1548. (b) Miyata, K.; Mineo, R.; Tamamushi, R.; Mizuta, M.; Ohkubo, A.; Taguchi, H.; Seio, K.; Santa, T.; Sekine. M. *J. Org. Chem.* **2007**, *72*, 102−108.

(11) (a) Takadate, A.; Masuda, T.; Murata, C.; Tanaka, T.; Irikura, M.; Goya, S. *Anal. Sci.* **1995**, *11*, 97−101. (b) Takadate, A.; Masuda, T.; Murata, C.; Isobe, A.; Shinohara, T.; Irikura, M.; Goya, S. *Anal. Sci.* **1997**, *13*, 753−756. (c) Takadate, A.; Masuda, T.; Murata, C.; Shibuya, M.; Isobe, A. *Chem. Pharm. Bull.* **2000**, *48*, 256−260. (d) Takechi, H.; Oda, Y.; Nishizono, N.; Oda, K.; Machida, M. *Chem. Pharm. Bull.* **2000**, *48*, 1702−1710.

(12) Kosower, E. M. *Acc. Chem. Res.* **1982**, *15*, 259−266.

(13) (a) Shah, M.; Thangaraj, K.; Soong, M. L.; Wolford, L. T.; Boyer, J. H.; Politzer, I. R.; Pavlopoulos, T. G. *Heteroat. Chem.* **1990**, *1*, 389−399. (b) Boyer, J. H.; Haag, A. M.; Sathyamoorthi, G.; Soong, M. L.; Thangaraj, K.; Pavlopoulos, T. G. *Heteroat. Chem.* **1993**, *4*, 39−49.

(14) Neumann, M. G.; Gehlen, M. H.; Encinas, M. V.; Allen, N. S.; Corrales, T.; Peinado, C.; Catalina, F. *J. Chem. Soc., Faraday Trans.* **1997**, *93*, 1517−1521.

(15) Tomoda, H.; Hirano, T.; Saito, S.; Mutai, T.; Araki, K. *Bull. Chem. Soc. Jpn.* **1999**, *72*, 1327−1334.

(16) Takamuki, Y.; Maki, S.; Niwa, H.; Ikeda, H.; Hirano, T. *Tetrahedron* **2005**, *61*, 10073−10080.

SCHEME 3. Preparation of *N*-Boc-indole-2-borate Derivatives (2a−f) and *N*-Boc-indole-2-trifluoroborate Derivatives (3a)

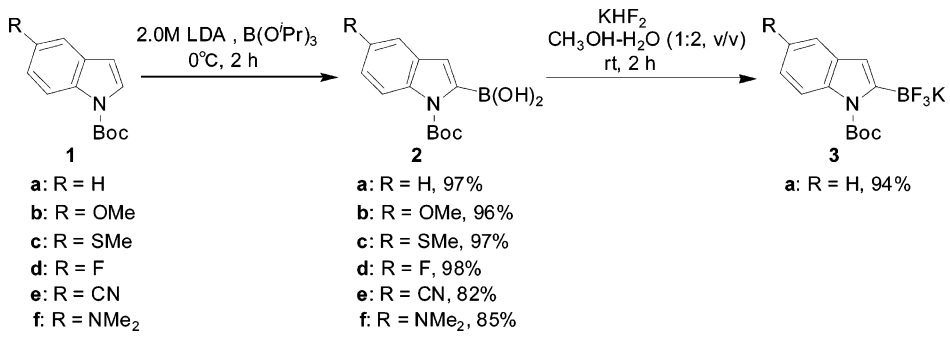

SCHEME 4. Synthesis of dC^{PPI} Derivatives (5a−f)

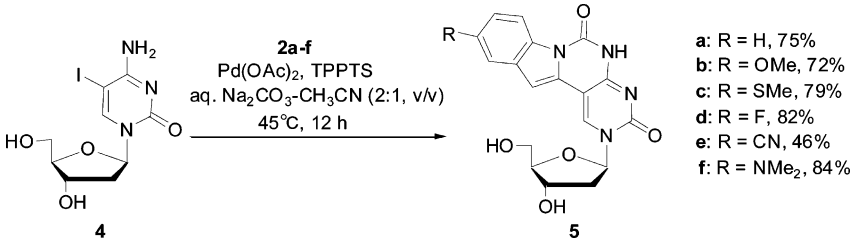

SCHEME 5. Synthesis of Sulfone (6) and Trimethylammonium (7) Derivatives

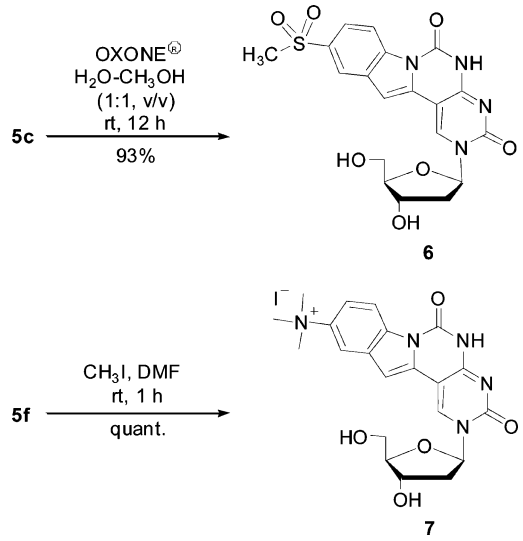

Results and Discussion

Synthesis of Pyrimidopyrimidoindole Nucleoside (dC^{PPI}) and Its Derivatives. We have already reported the synthesis of a deoxycytidine-based fluorescent nucleoside, pyrrolopyrimidopyrimidine nucleoside (dC^{PPP}), which was synthesized as outlined in Scheme 1.[10b] This compound was obtained in an attempt to synthesize 5-(pyrrol-2-yl)cytidine derivatives by a Suzuki−Miyaura coupling reaction of 5-iodo-2′-deoxycytidine with *N*-Boc-pyrrol-2-boronic acid. The initial coupling product was automatically cyclized with loss of *tert*-butyl alcohol to give dC^{ppp}. More interestingly, it was also found that dC^{PPP} had a high quantum yield of 0.11 in an aqueous buffer.

Therefore, we tried to synthesize dC^{PPP} derivatives having various substituents to clarify substitutent effects of this new fluorescent material. However, the synthesis of the corresponding *N*-Boc-pyrrole derivatives having a substituent at the 2- or 3-position was difficult because of their inherent instability. Therefore, we changed the structure of dC^{PPP} to the indole derivative dC^{PPI} having a benzene ring because borate derivatives of indole are more stable than those of pyrrole (Scheme 2).

To examine the substituent effect of dC^{PPI} at the 3-position, various *N*-Boc-indole-2-borates were synthesized, as shown in Scheme 3. The indole-2-borate building blocks (**2a**−**f**) could be readily prepared by addition of 1.3 equiv of LDA to a mixture of the *N*-Boc-indole derivative **1a**−**f**[17] and 1.5 equiv of triisopropyl borate at 0−5 °C. The other starting material of 5-iodo-2′-deoxycytidine was prepared according to the method reported in the literature.[18]

The borates (**2a**−**f**) thus obtained were allowed to react with the 5-iodo-2′-deoxycytidine (**4**) by a Suzuki−Miyaura-type reaction. Western et al.[19] have reported an aqueous-phase Suzuki−Miyaura coupling reaction of 8-bromo-2′-deoxyguanosine with arylboronic acids using a commercially available water-soluble phosphine ligand of tris(3-sulfonatophenyl)-phosphine (TPPTS). We applied this Suzuki−Miyaura coupling reaction to the synthesis of our compounds by use of a catalyst derived from TPPTS and palladium acetate. The reaction of 5-iodo-2′-deoxycytidine (**4**) with the *N*-Boc-indole-2-borate derivatives **2a**−**f** by use of 0.03 equiv of the catalyst in a water−acetonitrile solvent system (2:1, v/v) followed by the subsequent spontaneous cyclization gave the desired product (**5a**: dC^{PPI}) and its derivatives **5b**−**f** in 46% to 84% yields.

To examine the substituent effect in more detail, we synthesized two more compounds **6** and **7** by derivatization of **5c** and **5f**, respectively (Scheme 5). As shown in Scheme 5, the methylthio derivative **5c** could be converted to the sulfone derivative **6** in 93% yield by use of OXONE. Other oxidizing agents such as the H_5IO_6/CrO_3 system[20] were not effective because of the oxidation of the nitrogen atom in the cytosine

(17) Vazquez, E.; Davies, I. W.; Payack, J. F. *J. Org. Chem.* **2002**, *67*, 7551−7552.
(18) Chang, P. K.; Welch, A. D. *J. Med. Chem.* **1963**, *6*, 428−430.
(19) (a) Western, E. C.; Daft, J. R.; Johnson, E. M., II; Gannett, P. M.; Shaughnessy, K. H. *J. Org. Chem.* **2003**, *68*, 6767−6774. (b) Western, E. C.; Shaughnessy, K. H. *J. Org. Chem.* **2005**, *70*, 6378−6388.

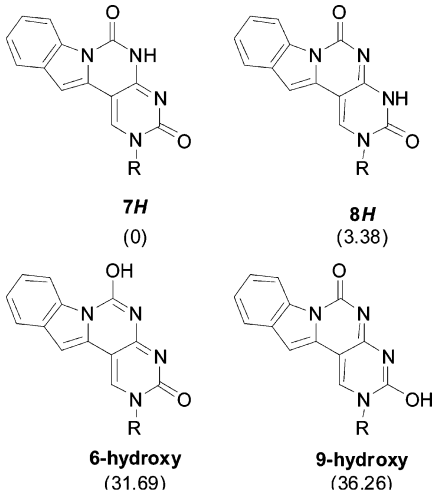

FIGURE 1. Four possible tautomers of the aglycon part of **5a**. The numbers in parentheses are the energy differences (kcal/mol) between the four isomers (R = CH_3) and that of the 7*H* isomer calculated at the B3LYP/6-31G* level.

ring. Moreover, the reaction of **5f** with 10 equiv of methyl iodide in *N*,*N*-dimethylformamide gave quantitatively the 3-trimethylammonium salt derivative **7**.

Determination of the Stable Tautomeric Structure of 5a in Solution. Prior to the spectroscopic studies, we tried to unambiguously determine the tautomeric form of the newly synthesized nucleosides by use of the simplest **5a** as a model compound. As shown in Figure 1, there are four possible tautomers in the aglycon part of **5a**, as shown in Figure 1. First of all, we carried out density functional calculations at the B3LYP/6-31G* level to compare the relative stability of the tautomers of the 1-methylated modified base (R = $-CH_3$) as the simplest compound in place of **5a**. According to the calculations, two enol-type tautomers of the 6- and 9-hydroxy derivatives were unstable by more than 30 kcal/mol in comparison with the 7*H* tautomer. These values suggested that the isomers containing the enol structures were not plausible as the major tautomers of **5a**. In contrast, the stability of 7*H* and 8*H* isomers differed by only 3.38 kcal/mol, and we could not establish which was the major isomer.

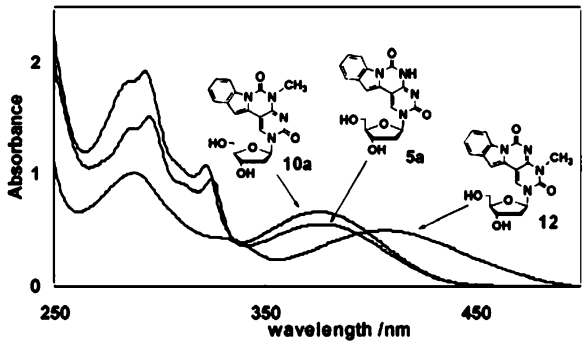

FIGURE 2. UV spectra of **5a**, **10a**, and **12** (0.1 mM) in 10 mM phosphate buffer (pH 7.4).

Therefore, we synthesized the 7-methyl (**10a**) and 8-methyl (**12**) derivatives of **5a** as the model compounds of the 7*H* and 8*H* isomers, respectively (Scheme 6). The 7-methyl derivative **10a** was successfully synthesized in 22% yield according to the synthetic scheme for **5a** by use of 5-iodo-4-*N*-methyl-2′-deoxycytidine (**9**) in place of **4**. In this case, a considerable amount of **10b** was formed because of the failure in the spontaneous cyclization. Next, we tried to synthesize the 8-methyl derivative **12** from 5-iodo-3-methyl-2′-deoxycytidine (**11**). Compound **11** could be obtained as a stable compound by the methylation of **4** followed by the purification by use of NH-silica gel chromatography. However, the Suzuki−Miyaura coupling of **11** with **2a** resulted in a very low yield of 37%. Therefore, we next examined the use of a more reactive trifluoroborate compound.[21] As shown in Scheme 3, the boronic acid derivative **2a** was converted to the trifluoroborate **3a** by treatment with an aqueous solution of KHF_2. Subsequently, compound **3a** was coupled with **11** to give the cross-coupling product in 60% yield.

To determine the major tautomer in aqueous and nonaqueous solutions, we measured the UV-absorption spectra of compounds **10a**, **12**, and **5a**. As shown in Figure 2, the UV spectra of compounds **5a** and **10a** measured in a phosphate buffer showed

SCHEME 6. Synthesis of 7-Methyl (10a) and 8-Methyl (12) Derivatives

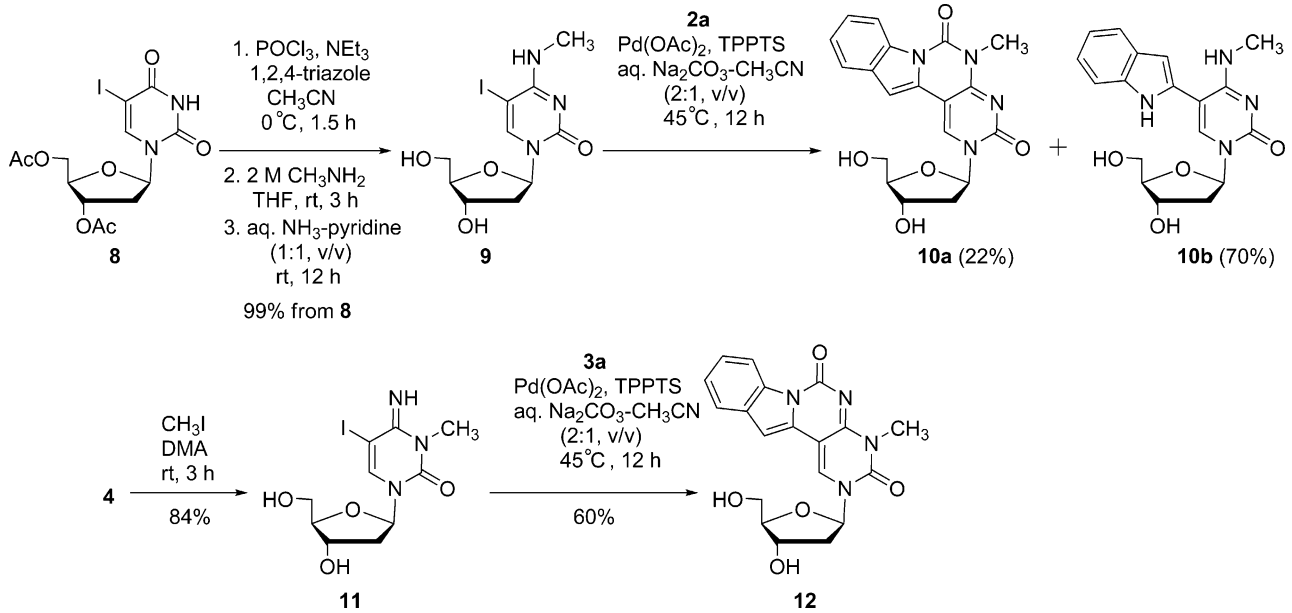

TABLE 1. Absorbance and Fluorescence Properties of dC^{PPI} Derivatives (5a−f, 6, 7) and dC^{PPP} in Buffer (pH 7.4)

	R	λ^{abs}_{max} [nm]	ϵ_{max} [$M^{-1}cm^{-1}$]	λ^{flu}_{max} [nm]	Stokes shift [nm]	Φ	Brightness $\epsilon_{max} \times \Phi$
5a	H	374	4157	513	139	0.006	25
5b	OMe	375	5321	511	136	0.005	27
5c	SMe	372	4110	511	139	0.002	8
5d	F	371	6284	505	134	0.019	119
5e	CN	369	6998	487	118	0.061	427
5f	NMe_2 (pH 7.0)	nd	nd[a]	489		<0.001	
5f	NMe_2 (pH 3.0)	366	9050	486	120	0.068	615
6	SO_2Me	367	7380	484	117	0.078	576
7	$N^+Me_3I^-$	368	8468	483	116	0.096	813
dC^{PPP}		369	4760	490	121	0.105	500

[a] nd: not determined.

the absorption maxima at very similar positions, 376 and 380 nm, respectively. Under the same conditions, the UV spectrum of compound **12** gave a significantly different absorption maximum at 407 nm. In nonaqueous solvents such as 1,4-dioxane, all the UV spectra of these compounds were essentially unchanged (data not shown) from those measured in the aqueous solvent. Therefore, it is reasonable to assume that compound **5a** exists in the 7*H* form in both aqueous and nonaqueous solutions. Because all of the newly synthesized nucleosides **5a**−**f** gave their absorption maxima at around 370 nm as described below, we concluded that all of the aglycon parts of **5a**−**f** exist in the 7*H* form.

Absorption and Emission Maxima of the dC^{PPP} and dC^{PPI} Derivatives. Photophysical properties of dC^{PPP}, dC^{PPI} (**5a**), and dC^{PPI} derivatives (**5b**−**f**, **6**, and **7**) are summarized in Table 1. Apparently, the differences in the chemical structure of the fluorophores showed only small effects on the wavelength of the absorption maxima, which were observed between 366 and 375 nm. We plotted the absorption maxima of **5a**−**f**, **6**, and **7** against the Hammett substituent parameters (σ^-),[22] as shown in Table S1 and Figure S1 in the Supporting Information. These results suggested that the substituent effect on the wavelength maxima correlated with the Hammett substituent parameter. It also turned out that the compounds having the larger σ values showed more red-shifted absorption maxima in both aqueous and nonaqueous solutions. In contrast, the molar absorption coefficients changed at most 2.2 times from 4110 to 9050 M^{-1} cm^{-1}.

Although the absorption maxima were rather insensitive to the alteration of the substituents on the indole ring, the emission maxima were more significantly influenced by the substituents in some cases. For example, although the absorption maximum of **5a** (R = H) and **5e** (R = CN) differed by only 5 nm, the emission maximum of them differed by 26, 513, and 487 nm, respectively. As a result, the Stokes shift became quite different depending on the chemical structure of the fluorophores as shown in the sixth column of Table 1. The compounds having the largest Stokes shift were **5a** and **5c** (139 nm), and the smallest was **7** (116 nm).

The substituents also affected the quantum yield (Φ) of these compounds. When the quantum yield of dC^{PPI} (**5a**, Φ = 0.006) was compared with that of dC^{PPP} (Φ = 0.105), it was clearly revealed that the addition of a benzene ring reduced the quantum yield of **5a** to 6% of that of dC^{PPP}. Interestingly, the introduction of the electron-withdrawing substituents such as fluoro (**5d**) and cyano (**5e**) groups recovered the quantum yields to 0.019 and 0.061, respectively. On the other hand, the introduction of the electron-donating groups having lone pairs such as methoxy (**5b**), methylthio (**5c**), and dimethylamino (**5f**) groups reduced the quantum yields to 0.005, 0.002, and <0.001, respectively.

Interestingly, the disappearance of the lone pairs of the methylthio derivative (**5c**) by oxidation resulted in a significant increase of the quantum yield, as shown by the quantum yield of the sulfone derivative **6** (Φ = 0.078). Similarly, the blockage of the lone pairs of the dimethylamino derivative **5f** by the protonation or alkylation gave a higher quantum yield of 0.068 (**5f**, pH 3.0) and 0.096 (**7**), respectively. These observations suggested that the weak fluorescence of the methoxy derivative **5b**, the methylthio derivative **5c**, and the dimethylamino derivatives (**5f**) was due to the results of quenching by the lone pairs on the oxygen, sulfur, and nitrogen atoms, respectively, probably through the PET mechanism.[23]

TABLE 2. Solvatochromic Data of 5a

solvent	ϵ^a	λ^{abs}_{max} [nm]	ϵ_{max} [$M^{-1}cm^{-1}$]	λ^{flu}_{max} [nm]	Stokes shift [nm]	Φ
benzene	2.3	372	5480	468	96	0.236
toluene	2.4	372	5230	467	95	0.234
$CHCl_3$	4.8	374	5210	479	105	0.199
CH_2Cl_2	8.9	372	5370	477	104	0.168
methanol	32.7	381	6930	488	108	0.114
CH_3CN	37.5	369	5410	472	103	0.221
DMF	36.7	373	6970	470	97	0.399
DMSO	46.7	373	7090	466	93	0.836

[a] Dielectric constants of the solvents

FIGURE 3. HOMO-1, HOMO, and LUMO molecular orbitals of the aglycon part of dC^{PPI} (R = H) calculated according to the DFT at the B3LYP/6-31G* level.

(20) Xu, L.; Cheng, J.; Trudell, M. L. *J. Org. Chem.* **2003**, *68*, 5388−5391.
(21) Molander, G. A.; Biolatto, B. *J. Org. Chem.* **2003**, *68*, 4302−4314.
(22) Hansch, C.; Leo, A.; Taft, R. W. *Chem. Rev.* **1991**, *91*, 165−195.
(23) (a) Ghosh, H. N.; Pal, H.; Palit, D. K.; Mukherjee, T.; Mittal, J. P. *J. Photochem. Photobiol. A* **1993**, *73*, 17−22. (b) Zallesskaya, G. A.; Yakovlev, D. L.; Sambor, E. G. *J. Appl. Spectrosc.* **2002**, *69*, 526−533. (c) Gorner, H. *Photochem. Photobiol.* **2003**, *77*, 171−179.

As described above, both the absorption coefficients (ϵ_{max}) and the quantum yields (Φ) were influenced by the substituents. Therefore, the brightness as an important property of the fluorophores was estimated by the ϵ_{max} and Φ values. The indexes are listed in the last column of Table 1. As shown in this table, the brightest was the trimethylammonium derivative **7**, which had a brightness index of 813. By comparing the brightness of **5a** (R = H) with that of the trimethylammonium derivative **7**, it was suggested that the fluorescent brightness of the dC^{PPI} derivatives could be enhanced up to 33 times. The sulfone derivative **6** also had large brightness values, 576, which were larger than that of the previously synthesized dC^{PPP}, which had a brightness of 500.

Origin of the Large Stokes Shifts Modeled by DFT Calculations. Experimentally, all compounds of this study showed large Stokes shifts (116−139 nm in buffer). In general, one of the major factors that would produce a very large Stokes shift is considered to be the solvent reorganization around the excited state dipole. Shown in Figure 3 is the relative distribution of HOMO, HOMO-1, and LUMO on the geometry-optimized ground state structure of the aglycon part of dC^{PPI} calculated at the B3LYP/6-31G* level. These models show that the HOMO and HOMO-1 extend to the indole part of the fluorophore and the LUMO locates mainly in the pyrimidopyrimidine part. These results indicate a considerable change of the molecular dipole moment vector, $\mu_e - \mu_g$, upon photoexcitation from the ground state to the excited state. It is expected that the large $\mu_e - \mu_g$ will lead to the reorganization of the solvation around the molecule giving rise to the large Stokes shifts.

Solvent Dependence of the Stokes Shifts of dC^{PPI} Derivatives. We examined the solvatochromism of dC^{PPI} derivatives. For this purpose, the absorption and emission spectra of **5a**−**f**, **6**, and **7** were measured in various solvents and the data were analyzed. Shown in Table 2 are example data for **5a**. The data for the other compounds are listed in Tables S2 and S3 in the Supporting Information. The data in Table 2 revealed the small but significant dependence of the absorption maximum on the solvents. In addition, the emission maxima were red-shifted from 467 nm in toluene to 488 nm in methanol as the solvent polarity was changed. The solvent dependence could be more quantitatively analyzed by plotting the emission maxima energies of **5a**−**e** against the solvent polarity $E_T(30)$[24] values, as shown in Table S4 and Figure S4 in the Supporting Information. For all compounds, the emission energies were almost unchanged in the solvents having the $E_T(30)$ values between 33.9 (toluene) and 45.6 (acetonitrile), and decreased when they were dissolved in more polar solvents such as water and methanol whose $E_T(30)$ values are 63.1 and 55.4, respectively. The bathochromic shift observed upon increasing the solvent polarity is suggestive of a greater stabilization of the excited state.

These solvent effects on the spectroscopic properties of **5a** could be put together into the Stokes shift parameters which are shown in the sixth column of Table 2. As shown in Figure S5 (Supporting Information), the Stokes shift parameters were dependent on the $E_T(30)$ values. Except for the aqueous solution, the Stokes shifts of all dC^{PPI} derivatives differed only slightly even if the solvent polarity was changed from toluene to methanol. In contrast, the Stokes shift observed in the aqueous solutions was signifcantly larger than those observed in the other solvents. These results suggested that the Stokes shifts of the dC^{PPI} derivatives could be used to monitor whether the derivatives were in the aqueous environment or not.

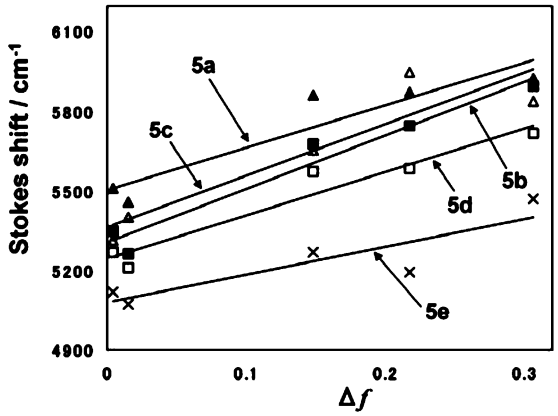

FIGURE 4. Solvatochromic shifts as a function of the solvent polarity parameter. Stokes shift (cm^{-1}) in different solvents vs Δf for dC^{PPI}: **5a** (R = H, closed triangle), **5b** (R = OMe, closed square), **5c** (R = SMe, open triangle), **5d** (R = F, open square), and **5e** (R = CN, crosses). Δf values are 0.005 (in benzene), 0.015 (in toluene), 0.149 (in $CHCl_3$), 0.218 (in CH_2Cl_2), and 0.306 (in CH_3CN), respectively.

TABLE 3. Slopes of the Solvatochromic Plots and Estimated Dipole Moments According to the Lippert−Mataga Model

	R	$2(\mu_e - \mu_g)^2/a_0^3$ [cm^{-1}][a]	a_0 [Å][b]	μ_g [D][c]	$\mu_e - \mu_g$ [D]	μ_e [D]
5a	H	1595	5.38	6.78	3.51	10.29
5b	OMe	2029	5.69	6.47	4.30	10.78
5c	SMe	1933	5.61	5.55	4.12	9.67
5d	F	1629	5.56	4.74	3.73	8.47
5e	CN	1062	5.74	5.23	3.16	8.39

[a] Slope of the solvatochromic plot (from eq 1 in the Experimental Section). [b] Onsager cavity radii a_0 were calculated from the molecular volumes based on geometry-optimized structures. [c] Computed ground-state dipole moment at the B3LYP/6-31G* level.

The photophysical data thus obtained can be analyzed further by considering the dipole−dipole interaction of the polarized excited state with solvents.[25] For this purpose we carried out another analysis of the solvatochromic effects by use of Lippert−Mataga formalism[26] in which the Stokes shifts [described in cm^{-1}] are plotted against the solvent polarity parameter difference, Δf. According to this theory, the solvatochromic effect could be analyzed by considering the polarity of the solvents, the dipole moment of the excited states of the fluorophores, and the molecular volumes of the fluorophores.

The results of the Lippert−Mataga analyses by use of the data of benzene, toluene, CH_2Cl_2, $CHCl_3$, and CH_3CN are shown in Figure 4 and are summarized in Table 3. The data for CH_3OH, DMF, and DMSO were not included in these plots because of the strong hydrogen bonding ability of these solvent molecules. Apparently, from the data in the second column of Table 3 which correspond to the slope of the linear regression analyses in Figure 4, the solvent dependence of the Stokes shift was the largest in the case of the methoxy derivative **5b**, and the smallest in the case of the cyano derivative **5e**. Accordingly,

(24) Reichardt, C. *Chem. Rev.* **1994**, *94*, 2319−2358.

(25) Lakowicz, J. R. *Principles of Fluorescence Spectroscopy*, 2nd ed.; Kluwer Academic: New York, 1999.

(26) (a) Mataga, N.; Kaifu, Y.; Koizumi, M. *Bull. Chem. Soc. Jpn.* **1955**, *28*, 690−691. (b) Mataga, N.; Kaifu, Y.; Koizumi, M. *Bull. Chem. Soc. Jpn.* **1956**, *29*, 465−470. (c) Mertz, E. L.; Tikhomirov, V. A.; Krishtalik, L. I. *J. Phys. Chem. A* **1997**, *101*, 3433−3442. (d) Würthner, F.; Ahmed, S.; Thalacker, C.; Debaerdemaeker, T. *Chem. Eur. J.* **2002**, *8*, 4742−4750.

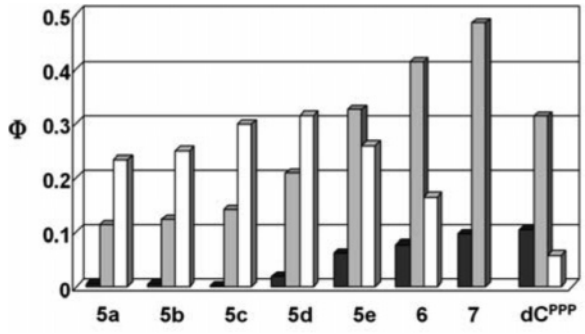

FIGURE 5. Comparison of the emission quantum yields in the buffer (black), methanol (gray), and toluene (white).

the order of the solvent dependence was R = cyano (**5e**) < fluoro (**5d**) < hydrogen (**5a**) < methylthio (**5c**) < methoxy (**5b**). Next, the slopes, thus obtained, were translated to the excited state dipole moments (μ_e) in combination with the quantum chemically calculated molecular volumes of the chromophores (a_0^3), the solvent polarity indexes (Δf) calculated from the dielectric constant of the solvent (ϵ_s), and the ground state dipole moment (μ_g) calculated quantum chemically. As a result, the μ_e of the methoxy derivative **5b** was estimated to be the largest, 10.78 D, and that of the cyano derivative **5e** was the smallest, 8.39 D. From these analyses, it was indicated that the excited state of **5b** has the largest dipole moment and must be solvated mostly by the dipole−dipole interaction with the solvent molecules. As stated above, the stabilization through solvation of this large dipole can lead to significant solvent reorganization and result in the large Stokes shifts.

Solvent Dependence of Quantum Yields. As described above, the Stokes shifts of dC^{PPI} derivatives were solvent dependent. It was also revealed that the quantum yield of these compounds was also strongly solvent dependent (Table 2, also Table S2 in the Supporting Information). For all the compounds, the quantum yield in the methanol solution was larger than that in the aqueous buffer. Interestingly, the dC^{PPI} derivatives could be clarified into two groups when the quantum yields in toluene were taken into consideration. As shown in Figure 5, compounds **5a** (R = H), **5b** (R = OMe), **5c** (R = SMe), and **5d** (R = F) form a group that showed larger quantum yields in less polar toluene than in more polar methanol. On the other hand, **5e** (R = CN), **6** (R = SO_2Me), and the previously reported dC^{PPP} form another group showing an opposite trend. Compound **7** (R = $N^+Me_3I^-$) could not be analyzed in toluene because of the very low solubility to this solvent. Such interesting properties could be described schematically by plotting the quantum yields against the Hammett constants (σ^-). As shown in Figure S6 (Supporting Information), in methanol, the quantum yields of the dC^{PPI} increased almost linearly as the σ^- of the substituents increased whereas it slightly decreased in toluene. Thus, the two lines crossed at the point whose σ^- value was nearly equal to 0.35. Therefore, the substituents could be divided into two groups across the σ^- value of 0.35. In other solvents such as benzene, $CHCl_3$, CH_2Cl_2, and CH_3CN, likewise methanol, the quantum yield of dC^{PPI} increased as Hammett constants increased (Table S2, Supporting Information).

It is well-known that the fluorescent nucleosides which change their fluorescence intensities depending on the polar or nonpolar environment around them can be used as probes for the local structures of nucleic acids. Previously, Ganesh et al. have shown that the major and the minor groove of DNA have the smaller dielectric constants ϵ of 40−60 and 22, respectively, in comparison to that of bulk water (ϵ = 80).[27] These data suggest that the polarity of the interior of DNA is close to that of methanol (ϵ = 32.7). In view of this, dC^{PPI} derivatives must be useful as the fluorescent structure probes for nucleic acids because of the large increase of the quantum yields upon change from an aqueous solvent to methanol. Among them, the brightest **7** (Table 1) must be the most useful as a new structural probe for nucleic acids.

Conclusion

The pyrimidopyrimidoindole nucleoside dC^{PPI} (**5a**) and its derivatives (**5b**−**f**, **6**, and **7**) were synthesized and their photophysical characters were evaluated. The fluorescent properties could be modulated by the introduction of various substituents. For example, the introduction of the substituents having lone pairs weakened the fluorescent intensity as exemplified by compounds **5b**, **5c**, and **5f**. Interestingly, blockage of the lone pairs by oxidation (**6**), alkylation (**7**), or protonation (**5f** at pH 3.0) recovered the fluorescence to such an extent that their brightness exceeded that of dC^{PPP}. In addition, introduction of the electron-withdrawing groups such as fluoro (**5d**) and cyano (**5e**) groups increased the brightness. We also evaluated the solvent dependence of the fluorescent quantum yields of dC^{PPI} (**5a**) and its derivatives. Despite their similar pyrimidopyrimidoindole structures, the derivatives could be categorized into two different groups. One includes compounds **5a** (R = H), **5b** (R = OMe), **5c** (R = SMe), and **5d** (R = F), and they have solvent-dependent quantum yields which are larger than those in polar methanol. On the other hand, **5e** (R = CN), **6** (R = SO_2Me), and the previously reported dC^{PPP} form another group showing an opposite trend. These solvent-dependent fluorescence properties indicated the usefulness of some of the fluorescent nucleosides reported in this paper as structure probes of nucleic acids.

Among all the newly synthesized fluorescent nucleosides, the trimethylammonium derivative **7** was the brightest. Development and application of this compound in the fluorescent analysis of DNAs and RNAs will be reported in due course.

Experimental Section

General Procedure for the Synthesis of *N*-Boc Indoles (1a−f): *N*-Boc-5-methylthioindole (1c). To a solution of 5-methylthioindole (3.7 g, 22.7 mmol) and *N*,*N*-dimetylaminopyridine (280 mg, 2.27 mmol) in CH_2Cl_2 (23 mL) was added Boc anhydride (5.9 g, 27.2 mmol). After being stirred at room temperature for 1 h, the mixture was washed with 1 M $KHSO_4$ and 1 M $NaHCO_3$. The organic layer was collected, dried over $MgSO_4$, filtered, and concentrated under reduced pressure. The resulting solid was purified by C-200 silica gel chromatography with $CHCl_3$ to give **1c** (5.9 g, 99%): ^{1}H NMR ($CDCl_3$) δ 1.66 (9H, s), 2.51 (3H, s), 6.50 (1H, d, J = 3.4 Hz), 7.28 (1H, dd, J = 1.7, 8.3 Hz), 7.49 (1H, d, J = 1.7 Hz), 7.58 (1H, d, J = 3.4 Hz), 8.05 (1H, d, J = 8.3 Hz); ^{13}C NMR ($CDCl_3$) δ 17.5, 27.4, 28.1, 106.7, 115.5, 120.1, 124.7, 126.5, 131.7. ESI-MS *m*/*z* calcd for $C_{14}H_{18}NO_2S$ [M + H] 264.1085, found 264.1143.

***N*-Boc-5-dimethylaminoindole (1f).** Compound **1f** was synthesized in 98% yield from 5-*N*,*N*-dimethylaminoindole according to

(27) (a) Jin, R.; Breslauer, K. J. *Proc. Natl. Acad. Sci. U.S.A.* **1988**, *85*, 8939−8942. (b) Barawkar, D. A.; Ganesh, K. N. *Nucleic Acids Res.* **1995**, *23*, 159−168. (c) Lamm, G.; Pack, G. R. *J. Phys. Chem.* **1997**, *101*, 959−965. (d) Young, M. A.; Jayaram, B.; Beveridge, D. L. *J. Phys. Chem.* **1998**, *102*, 7666−7669.

the general procedure. ^{1}H NMR (DMSO-d_6) δ 1.61 (9H, s), 2.89 (6H, s), 6.55 (1H, dd, J = 0.5, 3.7 Hz), 6.84−6.88 (2H, m), 7.54 (1H, d, J = 3.7 Hz), 7.85 (1H, d, J = 8.8 Hz); ^{13}C NMR (DMSO-d_6) δ 27.9, 41.3, 83.3, 103.9, 107.6, 112.0, 115.0, 126.1, 127.5, 131.4, 147.4, 149.3. ESI-MS m/z calcd for $C_{15}H_{21}N_2O_2$ [M + H] 261.1603, found 261.1528.

General Procedure for the Synthesis of *N*-Boc-indole-2-borate Derivatives: *N*-Boc-5-methylthioindole-2-borate (2c). To a solution of **1c** (0.5 g, 1.9 mmol) in THF (2.5 mL) was added triisopropyl borate (0.65 mL, 2.85 mmol). The solution was cooled to 0−5 °C in an ice bath, and LDA (2.0 M, 2.5 mmol) was added over 1 h. After 2 h, the reaction was poured into the phosphate buffer (pH 6.0). The organic layer was collected, dried over $MgSO_4$, and filtered. The filtrate was concentrated under reduced pressure. The residue was chromatographed on a column of silica gel (10 g) with chloroform. The fractions containing **2c** were concentrated under reduced pressure. The residue was precipitated from acetonitrile/water to give **2c** (0.57 g, 97%): ^{1}H NMR (DMSO-d_6) δ 1.59 (9H, s), 2.75 (3H, s), 6.57 (1H, s), 7.20 (1H, dd, J = 1.8, 8.6 Hz), 7.47 (1H ,d, J = 1.8 Hz), 8.00 (1H, d, J = 8.6 Hz), 8.21 (2H, s); ^{13}C NMR (DMSO-d_6) δ 16.1, 27.7, 84.3, 111.7, 115.1, 118.6, 123.5, 131.4, 131.7, 134.4, 149.9. ESI-MS m/z calcd for $C_{14}H_{19}BNO_4S$ [M + H] 308.1128, found 308.1149.

***N*-Boc-5-dimethylaminoindole-2-borate (2f).** Compound **2f** was synthesized in 85% yield from **1f** according to the general procedure. ^{1}H NMR (DMSO-d_6) δ 1.58 (9H, s), 2.88 (6H, s), 6.85 (1H, m), 6.80−6.82 (2H, m), 7.87 (1H, d, J = 8.8 Hz), 8.13 (2H, s); ^{13}C NMR (DMSO-d_6) δ 27.9, 41.4, 83.6, 103.4, 111.8, 112.6, 115.0, 129.2, 131.9, 147.4, 150.2. ESI-MS m/z calcd for $C_{15}H_{22}BN_2O_4$ [M + H] 305.1673, found 305.1605.

Potassium *N*-Boc-indole-2-trifluoroborate (3a). *N*-Boc-indole-2-borate (**2a**) (3.0 g, 11.5 mmol) and potassium hydrogen fluoride (2.24 g, 28.7 mmol) were vigorously stirred in a mixture of methanol (3.3 mL) and water (6.3 mL) for 2 h. The resulting amber solid was allowed to stand for 2 h at 4 °C and then filtered and washed with a minimum amount of cold methanol and 2-propanol. The solid was dried on a high-vacuum line to give **3a** (3.5 g, 94%): ^{1}H NMR (DMSO-d_6) δ 1.56 (9H, s), 6.39 (1H, s), 7.02−7.08 (2H, m), 7.37 (1H, d, J = 7.3 Hz), 8.01 (1H, d, J = 7.8 Hz); ^{13}C NMR (DMSO-d_6) δ 27.9, 81.5, 111.8, 114.7, 119.4, 121.4, 121.8, 130.9, 137.7, 151.6. ^{19}F NMR (DMSO-d_6) δ −136.7. Anal. Calcd for $C_{13}H_{14}BF_3KNO_2 \cdot {}^1/_5{}^i$PrOH: C, 48.73; H, 4.69; N, 4.18. Found: C, 49.00; H, 4.53; N, 4.42.

General Procedure for the Preparation of Pyrimidopyrimidoindole Nucleosides, dC^{PPI} Derivatives (5a−f): 10-(2-Deoxy-β-D-ribofuranosyl)pyrimido[4′,5′:4,5]pyrimido[1,6-*a*]indole-6,9-(7*H*)-dione (5a). Compound **4** (400 mg, 1.1 mmol), palladium acetate (7.6 mg, 0.03 mmol), TPPTS (51.4 mg, 0.09 mmol), Na_2CO_3 (264 mg, 2.5 mmol), and **2a** (590 mg, 2.3 mmol) were placed in a round-bottomed flask under argon. Degassed H_2O-CH_3CN (2:1, v/v, 11 mL) was added, and the mixture was stirred at 45° C for 12 h. The mixture was evaporated under reduced pressure. The crude product was purified by C-200 silica gel chromatography with $CHCl_3$−MeOH to give **5a** (312 mg, 75%): ^{1}H NMR (DMSO-d_6) δ 2.19−2.40 (2H, m), 3.70−3.86 (2H, m), 3.92−3.93 (1H, m), 4.30−4.34 (1H, dd, J = 5.1, 10.3 Hz), 5.32 (1H, d, J = 4.4 Hz), 5.51 (1H, t, J = 4.6 Hz), 6.16 (1H, t, J = 5.7 Hz), 6.96 (1H, s), 7.31−7.34 (2H, m), 7.64−7.66 (1H, m), 8.37−8.39 (1H, m), 9.37 (1H, s), 11.99 (1H, s); ^{13}C NMR (DMSO-d_6) δ 41.3, 60.2, 68.7, 86.9, 87.9, 95.8, 97.4, 115.3, 120.2, 123.5, 124.1, 130.1, 130.4, 133.4, 140.5, 147.5, 153.5, 157.7. Anal. Calcd for $C_{18}H_{16}N_4O_5 \cdot {}^1/_2H_2O$: C, 57.29; H, 4.54; N, 14.85. Found: C, 57.38; H, 4.50; N, 14.53.

3-Methoxy-10-(2-deoxy-β-D-ribofuranosyl)pyrimido[4′,5′:4,5]-pyrimido[1,6-*a*]indole-6,9(7*H*)-dione (5b). Compound **5b** was synthesized in 72% yield from **2b** according to the general procedure. ^{1}H NMR (DMSO-d_6) δ 2.22−2.37 (2H, m), 3.68−3.84 (2H, m), 3.81 (3H, s), 3.91−3.92 (1H, m), 4.31 (1H, dd, J = 5.1, 10.4 Hz), 5.31 (1H, d, J = 4.6 Hz), 5.55 (1H, m), 6.17 (1H, t, J = 5.8 Hz), 6.86 (1H, s), 6.91 (1H, d, J = 9.0 Hz), 7.13 (1H, s), 8.26 (1H, d, J = 9.0 Hz), 9.29 (1H, s), 11.95 (1H, s); ^{13}C NMR (DMSO-d_6) δ 41.3, 55.5, 60.3, 68.8, 86.8, 87.9, 96.2, 96.8, 102.5, 111.9, 115.9, 128.0, 131.1, 131.2, 139.8, 148.1, 153.6, 156.4, 158.6. ESI-MS m/z calcd for $C_{19}H_{18}N_4NaO_6$ [M + Na] 421.1124, found 421.1297.

3-Methylthio-10-(2-deoxy-β-D-ribofuranosyl)pyrimido[4′,5′:4,5]pyrimido[1,6-*a*]indole-6,9(7*H*)-dione (5c). Compound **5c** was synthesized in 79% yield from **2c** according to the general procedure. ^{1}H NMR (DMSO-d_6) δ 2.18−2.39 (2H, m), 3.69−3.85 (2H, m), 3.92 (1H, dd, J = 3.2, 7.6 Hz), 4.31 (1H, dd, J = 5.1, 10.3 Hz), 5.33 (1H, d, J = 4.4 Hz), 5.48 (1H, t, J = 4.7 Hz), 6.16 (1H, t, J = 5.6 Hz), 6.88 (1H, s), 7.23 (1H, dd, J = 1.7, 8.5 Hz), 7.52 (1H, d, J = 1.5 Hz), 8.30 (1H, d, J = 8.5 Hz), 9.32 (1H, s), 12.0 (1H, s); ^{13}C NMR (DMSO-d_6) δ 15.9, 41.2, 60.2, 68.8, 87.0, 87.9, 95.8, 96.8, 115.5, 117.5, 122.6, 131.0, 131.3, 133.2, 140.6, 147.2, 153.4, 157.6. ESI-MS m/z calcd for $C_{19}H_{18}N_4NaO_5S$ [M + Na] 437.0896, found 437.0970.

3-Fluoro-10-(2-deoxy-β-D-ribofuranosyl)pyrimido[4′,5′:4,5]-pyrimido[1,6-*a*]indole-6,9(7*H*)-dione (5d). Compounds **5d** were synthesized in 82% yield from **2d** according to the general procedure. ^{1}H NMR (DMSO-d_6) δ 2.18−2.40 (2H, m), 3.69−3.85 (2H, m), 3.92 (1H, dd, J = 3.2, 7.8 Hz), 4.31 (1H, dd, J = 5.2, 10.5 Hz), 5.32 (1H, d, J = 4.6 Hz), 5.49 (1H, t, J = 4.7 Hz), 6.16 (1H, t, J = 5.7 Hz), 6.95 (1H, s), 7.15 (1H, dd, J = 2.4, 9.2 Hz), 7.45 (1H, dd, J = 2.4, 9.2 Hz), 8.37 (1H, dd, J = 4.7, 8.9 Hz), 9.36 (1H, s), 12.05 (1H, s); ^{13}C NMR (DMSO-d_6) δ 41.3, 60.2, 68.7, 87.0, 88.0, 95.7, 97.2, 105.6, 111.1, 116.5, 130.0, 131.3, 132.3, 141.0, 147.3, 153.5, 158.1, 160.3. ESI-MS m/z calcd for $C_{18}H_{15}FN_4NaO_5$ [M + Na] 409.0924, found 409.0925.

3-Cyano-10-(2-deoxy-β-D-ribofuranosyl)pyrimido[4′,5′:4,5]pyrimido[1,6-*a*]indole-6,9(7*H*)-dione (5e). Compound **5e** was synthesized in 46% yield from **2e** according to the general procedure. ^{1}H NMR (DMSO-d_6) δ 2.22−2.41 (2H, m), 3.69−3.85 (2H, m), 3.93 (1H, dd, J = 3.3, 7.7 Hz), 4.31 (1H, dd, J = 5.3, 10.8 Hz), 5.32 (1H, d, J = 4.6 Hz), 5.49 (1H, t, J = 4.9 Hz), 6.16 (1H, t, J = 5.8 Hz), 7.04 (1H, s), 7.70 (1H, dd, J = 1.5, 8.5 Hz), 8.20 (1H, d, J = 1.2 Hz), 8.53 (1H, d, J = 8.5 Hz), 9.39 (1H, s), 12.21 (1H, s); ^{13}C NMR (DMSO-d_6) δ 41.2, 60.3, 68.8, 87.0, 88.0, 95.7, 96.6, 106.1, 116.2, 119.8, 124.9, 126.1, 130.2, 133.2, 135.2, 141.1, 148.0, 153.5, 158.4. ESI-MS m/z calcd for $C_{19}H_{15}N_5NaO_5$ [M + Na] 416.0971, found 416.0979.

3-*N*,*N*-Dimethylamino-10-(2-deoxy-β-D-ribofuranosyl)pyrimido-[4′,5′:4,5]pyrimido[1,6-*a*]indole-6,9(7*H*)-dione (5f). Compound **5f** was synthesized in 84% yield from **2f** according to the general procedure. ^{1}H NMR (DMSO-d_6) δ 2.08−2.39 (2H, m), 2.93 (6H, s), 3.69−3.85 (2H, m), 3.92(1H, dd, J = 3.2, 7.6 Hz), 4.31 (1H, dd, J = 5.2, 10.5 Hz), 5.31 (1H, d, J = 4.6 Hz), 5.47 (1H, t, J = 4.8 Hz), 6.16 (1H, t, J = 5.2 Hz), 6.81−6.87 (3H, m), 8.16 (1H, d, J = 3.4 Hz), 9.31 (1H, s), 11.85 (1H, s); ^{13}C NMR (DMSO-d_6) δ 41.1, 41.3, 60.2, 68.7, 86.9, 87.9, 96.1, 97.4, 102.2, 111.1, 115.5, 126.1, 130.2, 131.3, 140.1, 147.1, 148.3, 153.5, 157.6. ESI-MS m/z calcd for $C_{20}H_{22}N_5O_5$ [M + H] 412.1621, found 412.1670.

3-Methylsulfonyl-10-(2-deoxy-β-D-ribofuranosyl)pyrimido-[4′,5′:4,5]pyrimido[1,6-*a*]indole-6,9(7*H*)-dione (6). To a stirred solution of **5c** (0.06 mmol, 25 mg) in H_2O-CH_3OH (1:1, v/v, 4 mL) was added OXONE (0.18 mmol, 111 mg) at room temperature. After 12 h, the reaction was diluted with water and extracted with chloroform. The combined organic layers were washed with water and brine, dried over $MgSO_4$, and concentrated under reduced pressure. The crude product was purified by C-200 silica gel chromatography with $CHCl_3$−MeOH to give **6** (25 mg, 93%): ^{1}H NMR (DMSO-d_6) δ 2.21−2.40 (2H, m), 3.24 (3H, s), 3.70−3.85 (2H, m), 3.91−3.93 (1H, m), 4.31−4.33 (1H, m), 5.31 (1H, d, J = 4.6 Hz), 5.47 (1H, m), 6.17 (1H, t, J = 5.8 Hz), 7.09 (1H, s), 7.82−7.84 (1H, m), 8.20 (1H, d, J = 1.5 Hz), 8.61 (1H, d, J = 8.8 Hz), 9.37 (1H, s); ^{13}C NMR (DMSO-d_6) δ 41.2, 44.3, 45.9, 60.3, 68.8, 87.0, 87.9, 95.8, 97.1, 115.8, 119.4, 121.3, 130.0, 133.3, 135.6,

136.2, 141.0, 148.0, 153.0. Anal. Calcd for $C_{19}H_{18}N_4O_7S$: C, 51.12; H, 4.06; N, 12.55. Found: C, 51.36; H, 4.13; N, 12.42.

3-Trimethylammoniumiodido-10-(2-deoxy-β-D-ribofuranosyl)-pyrimido[4′,5′:4,5]pyrimido[1,6-*a*]indole-6,9(7*H*)-dione (7). To a stirred solution of **5f** (0.05 mmol, 20 mg) in *N*,*N*-dimethylformamide (1 mL) was added CH_3I (0.5 mmol, 31 μL). The mixture was then stirred for 10 min at 0 °C. The solution was allowed to warm to room temperature. After 1 h, the reaction was concentrated under reduced pressure to give **7** (27 mg, quant): ^{1}H NMR (DMSO-d_6) δ 2.22−2.43 (2H, m), 3.68 (9H, s), 3.70−3.86 (2H, m), 3.93−3.96 (1H, dd, J = 3.2, 8.8 Hz), 4.29−4.33 (1H, dd, J = 5.1, 10.3 Hz), 5.32 (1H, d, J = 4.4 Hz), 5.48 (1H, t, J = 5.0 Hz), 6.16 (1H, t, J = 5.8 Hz), 7.05 (1H, s), 7.90−7.93 (1H, dd, J = 2.7, 9.3 Hz), 8.23 (1H, d, J = 2.4 Hz), 8.49 (1H, d, J = 9.3 Hz), 9.43 (1H, s); ^{13}C NMR (DMSO-d_6) δ 41.2, 57.1, 60.3, 68.7, 87.3, 88.1, 95.5, 97.3, 112.2, 115.3, 115.9, 130.4, 132.8, 133.1, 141.5, 143.5, 147.4, 153.3, 157.7. Anal. Calcd for $C_{21}H_{24}IN_5O_5 \cdot {}^1/_4CHCl_3 \cdot {}^3/_4H_2O$: C, 42.77; H, 4.35; N, 11.74. Found: C, 42.82; H, 4.26; N, 11.84.

5-Iodo-4-*N*-methyl-2′-deoxycytidine (9). 1,2,4-Triazole (10.7 g, 154 mmol) was dissolved in CH_3CN (85 mL). The suspension was cooled to 0 °C and 3.1 mL (34.4 mmol) of $POCl_3$ was added dropwise. The mixture was stirred for 10 min, and then triethylamine (21.5 mL, 154 mmol) was added. To this solution was added **8** (5 g, 11.4 mmol). The solution was allowed to warm to room temperature. The reaction mixture was stirred for 30 min, followed by quenching with H_2O. The aqueous layer was separated and extracted twice with $CHCl_3$. The organic layer was washed with saturated $NaHCO_3$ solution, dried over $MgSO_4$, and concentrated under reduced pressure. To the residue was added 2 M methylamine in THF (30 mL), and the mixture was stirred at room temperature for 3 h. The solvents were removed under reduced pressure, and the residue was dissolved in pyridine (65 mL). To this solution was added concentrated NH_4OH (65 mL), and the mixture was stirred at room temperature for 12 h. The solvent was removed under reduced pressure, and the residue was purified by chromatography on a silica gel column with 10% methanol in $CHCl_3$, to give **9** (4.17 g, 99%): ^{1}H NMR (DMSO-d_6) δ 1.96−2.14 (2H, m), 2.78 (3H, d, J = 4.4 Hz), 3.53−3.63 (2H, m), 3.77 (1H, dd, J = 3.4, 6.8 Hz), 4.19−4.21 (1H, m), 5.05−5.25 (2H, br), 6.08 (1H, t, J = 6.5 Hz), 7.03 (1H, m), 8.24 (1H, s); ^{13}C NMR (DMSO-d_6) δ 28.6, 40.9, 58.0, 61.0, 70.1, 85.3, 87.5, 146.2, 153.9, 161.4. ESI-MS m/z calcd for $C_{10}H_{15}IN_3O_4$ [M + H] 368.0107, found 368.0255.

10-(2-Deoxy-β-D-ribofuranosyl)-7-methylpyrimido[4′,5′:4,5]-pyrimido[1,6-*a*]indole-6,9-dione (10a) and 5-(Indole-2-yl)-4-*N*-methyl-2′-deoxycytidine (10b). In a manner similar to that described for the synthesis of **5a**, a mixture of **9** (200 mg, 0.54 mmol) and **2a** (426 mg, 1.6 mmol) was treated with $Pd(OAc)_2$ (3.7 mg, 0.016 mmol), TPPTS (24.7 mg, 0.044 mmol), and Na_2CO_3 (127 mg, 1.2 mmol) to give **10a** (45 mg, 22%) and **10b** (136 mg, 70%). **10a**: ^{1}H NMR (DMSO-d_6) δ 2.19−2.42 (2H, m), 3.50 (3H, s), 3.72−3.87 (2H, m), 3.92−3.93 (1H, m), 4.33 (1H, dd, J = 5.5, 10.9 Hz), 5.51 (2H, br), 6.17 (1H, t, J = 5.5 Hz), 6.95 (1H, s), 7.33−7.34 (2H, m), 7.65 (1H, t, J = 4.3 Hz), 8.40 (1H, t, J = 4.5 Hz), 9.41 (1H, s); ^{13}C NMR (DMSO-d_6) δ 28.8, 41.3, 60.1, 68.5, 86.9, 87.9, 96.5, 97.1, 115.3, 120.2, 123.5, 124.2, 129.2, 130.0, 133.6, 140.2, 147.7, 153.2, 156.9. Anal. Calcd for $C_{19}H_{18}N_4O_5$: C, 59.68; H, 4.74; N, 14.65. Found: C, 59.63; H, 4.68; N, 14.46. **10b**: ^{1}H NMR (DMSO-d_6) δ 2.07−2.18 (2H, m), 2.80 (3H, d, J = 4.6 Hz), 3.50−3.59 (2H, m), 3.78−3.80 (1H, dd, J = 3.7, 7.1 Hz), 4.22−4.26 (1H, dd, J = 3.5, 9.5 Hz), 4.92 (1H, t, J = 5.1 Hz), 5.21 (1H, d, J = 4.2 Hz), 6.25 (1H, t, J = 6.7 Hz), 6.49 (1H, d, J = 1.2 Hz), 7.00 (1H, t, J = 7.6 Hz), 7.05−7.08 (1H, dd, J = 4.4, 9.0 Hz), 7.09−7.12 (1H, m), 7.37 (1H, d, J = 7.8 Hz), 7.53 (1H, d, J = 7.8 Hz), 7.93 (1H, s), 11.24 (1H, s); ^{13}C NMR (DMSO-d_6) δ 28.2, 40.6, 61.4, 70.5, 85.2, 87.5, 101.1, 101.7, 111.5, 119.4, 120.1, 121.5, 128.5, 130.5, 136.7, 139.5, 154.4, 161.5. ESI-MS m/z calcd for $C_{18}H_{20}N_4NaO_4$ [M + Na] 379.1382, found 379.1148.

5-Iodo-3-methyl-2′-deoxycytidine (11). Compound **4** (400 mg, 1.1 mmol) was dissolved in 2.3 mL of *N*,*N*-dimethylacetamide (DMA). To this solution was added methyl iodide (0.23 mL, 4.5 mmol) in DMA (4.5 mL). The reaction was run at room temperature. After 6 h the DMA was removed under vacuum, The residue was purified by chromatography on a NH-silica gel column with 6% methanol in $CHCl_3$ to give **11** (350 mg, 84%): ^{1}H NMR (DMSO-d_6) δ 2.05−2.09 (2H, m), 3.37 (3H, s), 3.53−3.61 (2H, m), 3.76−3.77 (1H, m), 4.22 (1H, m), 5.11 (1H, t, J = 4.9 Hz), 5.22 (1H, d, J = 4.2 Hz), 6.12 (1H, t, J = 6.7 Hz), 7.08 (1H, s), 7.98 (1H, s); ^{13}C NMR (DMSO-d_6) δ 30.7, 40.3, 61.2, 70.4, 70.5, 85.2, 87.5, 137.4, 150.0, 156.4. ESI-MS m/z calcd for $C_{10}H_{15}IN_3O_4$ [M + H] 368.0107, found 367.9944.

10-(2-Deoxy-β-D-ribofuranosyl)-8-methylpyrimido[4′,5′:4,5]-pyrimido[1,6-*a*]indole-6,9-dione (12). In a manner similar to that described for the synthesis of **5a**, the mixture of **11** (1.0 g, 2.7 mmol) and **3a** (2.84 g, 11 mmol) was treated with $Pd(OAc)_2$ (18.3 mg, 0.082 mmol), TPPTS (124 mg, 0.22 mmol), and Na_2CO_3 (634 mg, 6.0 mmol) to give **12** (410 mg, 60%): ^{1}H NMR (DMSO-d_6) δ 2.33−2.39 (2H, m), 3.50 (3H, s), 3.71−3.87 (2H, m), 3.91−3.93 (1H, m), 4.34 (1H, dd, J = 5.9, 11.0 Hz), 5.43 (1H, br), 5.65 (1H, br), 6.20 (1H, t, J = 5.6 Hz), 6.95 (1H, s), 7.28−7.32 (2H, m), 7.63 (1H, m), 8.46−8.48 (1H, m), 9.28 (1H, s); ^{13}C NMR (DMSO-d_6) δ 30.2, 41.0, 60.1, 68.6, 87.4, 88.0, 96.6, 98.4, 115.8, 120.2, 123.2, 123.8, 129.8, 131.1, 135.3, 148.5, 153.1, 158.4. Anal. Calcd for $C_{19}H_{18}N_4O_5 \cdot {}^1/_4CHCl_3$: C, 56.09; H, 4.46; N, 13.59. Found: C, 55.96; H, 4.75; N, 13.48.

Fluorescence Experiments. Fluorescence spectra were obtained at 25 °C in a 1 cm path length cell. The fluorescence quantum yield (Φ) was determined by use of 0.1 M quinine as a reference with the known Φ value of 0.53 in H_2SO_4.[28] The quantum yield was calculated according to the following equation:

$$\frac{\Phi_{F(S)}}{\Phi_{F(R)}} = \frac{A_{(S)}}{A_{(R)}} \frac{(Abs)_{(R)}}{(Abs)_{(S)}} \frac{{n_{(S)}}^2}{{n_{(R)}}^2}$$

Here, $\Phi_{F(S)}$ and $\Phi_{F(R)}$ are the fluorescence quantum yields of the sample and the reference, respectively, $(Abs)_{(S)}$ and $(Abs)_{(R)}$ are the respective optical density of the sample and the reference solutions at the wavelength of excitation, and $n_{(S)}$ and $n_{(R)}$ are the values of the refractive index for the respective solvents.

Lippert−Mataga Plots. The absorption and emission spectra of dC^{PPI} (R = H, OMe, SMe, F, CN) were acquired in five solvents (benzene, toluene, CH_2Cl_2, $CHCl_3$, and acetonitrile). The data for all absorption and emission spectra are given in Table S3 (Supporting Information).

The results could be quantitatively analyzed by use of the dipole interaction theory of Lippert and Mataga. The analysis of the Stokes shifts as a function of solvent polarity gives an estimate of the difference between excited state and ground state dipole moments. According to the Lippert−Mataga formalism, a plot of the Stokes shift $\Delta\nu$ ($\nu_{abs} - \nu_{em}$) versus the solvent polarity function $\Delta f = f(\epsilon_s) - f(n)$ allows for determination of the difference between the excited state and the ground state dipole moments ($\mu_e - \mu_g$) via linear regression:

$$\Delta\bar{\nu} = \bar{\nu}_{abs} - \bar{\nu}_{em} = \Delta\bar{\nu}_0 + \frac{2}{hc}\frac{(\mu_e - \mu_g)^2}{{a_0}^3}\Delta f \qquad (1)$$

with

$$\Delta f = f(\epsilon_s) - f(n) = \frac{\epsilon_s - 1}{2\epsilon_s + 1} - \frac{n^2 - 1}{2n^2 + 1}$$

The experimental data (Table S3, Supporting Information) were fitted to the above equation and the excited state dipole moments

(28) Adams, M. J.; Highfield, J. G.; Kirkbright, G. F. *Anal. Chem.* **1977**, *49*, 1850−1852.

(μ_e) were calculated by use of the slope of the experimental data, the quantum chemically calculated molecular volumes of the chromophores (a_0^3), the index values (Δf) calculated from the dielectric constant of the solvent (ϵ_s), and the ground state dipole moments (μ_g).

Computational Methods. The Gaussian 98 program package[29] was used for density functional theory (DFT) calculations to optimize the geometries and calculate the HOMO and LUMO energies as well as the dipole moments of the molecules. The cavity radius for each of the compounds was estimated based on the corresponding geometry-optimized structure and Monte Carlo integration of the volume inside a contour of 0.001 electrons/bohr^3 density (B3LYP/6-31G(d)//B3LYP/6-31G(d)).

Acknowledgment. This work was supported by Grant-in-Aid of CREST of JST (Japan Science and Technology) and the Ministry of Education, Science, Sports and Culture, Grant-in-aid for Scientific Research (A). This study was also supported by the Industrial Technology Research Grant Program in '05 from the New Energy and Industrial Technology Development Organization (NEDO) of Japan.

Supporting Information Available: Relationship between the absorption maximum of the **5a**−**f, 6**, and **7** and the Hammett substituent parameter (σ^-) (Table S1 and Figure S1), the solvatochromic data of **5b**−**e**, **6**, and **7** (Table S2), the photophysical date of **5a**−**e** (Table S3), the absorption spectra of **5a**−**e, 6**, and **7** (Figure S2), the fluorescence spectra of **5a**−**e**, **6**, and **7** (Figure S3), the relationship between emission energy and $E_T(30)$ values (Table S4 and Figure S4), and the ^{1}H NMR and ^{13}C NMR spectra of all the new products. This material is available free of charge via the Internet at http://pubs.acs.org.

JO070206J

(29) Frisch, M. J.; Trucks, G. W.; Schlegel, H. B.; Scuseria, G. E.; Robb, M. A.; Cheeseman, J. R.; Zakrzewski, V. G.; Montgomery, J. A., Jr.; Stratmann, R. E.; Burant, J. C.; Dapprich, S.; Millam, J. M.; Daniels, A. D.; Kudin, K. N.; Strain, M. C.; Farkas, O.; Tomasi, J.; Barone, V.; Cossi, M.; Cammi, R.; Mennucci, B.; Pomelli, C.; Adamo, C.; Clifford, S.; Ochterski, J.; Petersson, G. A.; Ayala, P. Y.; Cui, Q.; Morokuma, K.; Malick, D. K.; Rabuck, A. D.; Raghavachari, K.; Foresman, J. B.; Cioslowski, J.; Ortiz, J. V.; Stefanov, B. B.; Liu, G.; Liashenko, A.; Piskorz, P.; Komaromi, I.; Gomperts, R.; Martin, R. L.; Fox, D. J.; Keith, T.; Al-Laham, M. A.; Peng, C. Y.; Nanayakkara, A.; Gonzalez, C.; Challacombe, M.; Gill, P. M. W.; Johnson, B. G.; Chen, W.; Wong, M. W.; Andres, J. L.; Head-Gordon, M.; Replogle, E. S.; Pople, J. A. *Gaussian 98*, revision A.7; Gaussian, Inc.: Pittsburgh, PA, 1998.